AJNR Am J Neuroradiol 21:1470–1477, September 2000

Case Report

Colloid Cyst of the Third Ventricle: Imaging-pathologic Correlation

Diane Armao, Mauricio Castillo, Hong Chen, and Lester Kwock

Summary: Colloid cysts are relatively rare intracranial lesions located in the rostral aspect of the third ventricle. They may produce acute hydrocephalus, brain herniation, and lead to death. Although the clinical and imaging features of colloid cysts are well known, their etiology and the factors responsible for their imaging features continue to be a subject of debate. We present the imaging-pathologic correlation of a patient with a colloid cyst as well as data supporting the fact that the presence of cholesterol is probably responsible for the MR imaging features exhibited by some colloid cysts.

Colloid cysts are rare intracranial lesions occurring in approximately three individuals per million per year (1). Clinical symptoms may be intermittent, self-resolving, and nonspecific. Some colloid cysts result in acute onset of hydrocephalus and may lead to sudden death. The most common imaging finding is that of a rounded mass in the anterior aspect of the third ventricle. On CT scans, the lesions are often hyperdense, and their MR imaging features are variable (2). We present the clinical and imaging findings in a patient with a colloid cyst, and provide a gross anatomic and histopathologic correlation.

Case Report

The patient was a 36-year-old woman with a medical history significant for AIDS with multiple opportunistic infections, including *Pneumocystis carinii* and *Mycobacterium kanasii* pneumonias, cerebral toxoplasmosis, and cryptococcal meningitis as well as a history of a colloid cyst of the third ventricle detected by CT (Fig 1A). She had recently been admitted to an outside hospital for unexplained fever and painful lower-extremity edema. During treatment for acute-onset renal failure, the patient developed headache and nuchal rigidity. The CT scan was interpreted as stable. Antibiotic therapy for meningitis was initiated, and the headache and nuchal rigidity resolved. Progressive renal failure prompted transfer to our hospital for possible hemodyalysis. Shortly after transfer, the patient developed nuchal rigidity and deterioration of her mental status. Physical examination was noteworthy for a Cushing response (hypertension with bradycardia), bilaterally nonreactive and small pupils (<1mm), decorticate rigidity, positive oculocephalic movements and extensor plantar reflexes. An emergency noncontrast CT scan of the head showed hydrocephalus (Fig 1B). The patient was intubated and continued on broad-spectrum antibiotic therapy. An emergency ventriculostomy was performed, which relieved the increased intracranial pressure. Postoperative CT showed decompression of only one ventricle (Fig 1C). Another ventriculostomy was inserted (Fig 1D). Despite appropriate medical therapy, the patient's neurologic function continued to decline. Two additional ventriculostomies yielded no clinical benefit. Owing to the absence of cortical activity and poor prognosis, life support was withdrawn, and the patient expired 7 days after last admission. A general autopsy examination revealed HIV nephropathy and positive lung cultures for cytomegalovirus. Neuropathologic examination showed a colloid cyst of the third ventricle and HIV encephalitis. The underlying cause of death was acute obstuctive hydrocephalus with uncal herniation, secondary to a colloid cyst of the third ventricle.

Received February 21, 2000; accepted after revision April 10.

From the Departments of Radiology (D.A., M.C., L.K.) and Pathology and Laboratory Medicine (H.C.), University of North Carolina, Chapel Hill, NC 27599.

Address reprint requests to Mauricio Castillo, CB # 7510, UNC-CH, Chapel Hill, NC 27599-7510.

Imaging Studies

Initial noncontrast CT of the head showed dilatation of the lateral ventricles and brain atrophy (Fig 1). The colloid cyst had a rounded configuration and was hyperdense. After autopsy, the fixed brain was placed in a water bath and taken to the MR imaging unit. On the T1-weighted images, the lesion showed a central signal intensity slightly higher than that of the surrounding brain with a mildly hypointense rim (Fig 2A). On proton density–weighted images, the colloid cyst was of homogeneous signal intensity, and on T2-weighted images, it showed a central region of hypointensity surrounded by a rim of relative hyperintensity (similar to that of white matter) (Figs 2B and C). The T2-weighted appearance was a reversal of that seen on the T1-weighted study. The colloid cyst appeared slightly oval on this projection.

Neuropathologic Studies

Postmortem gross evaluation of the 2-week formalin-fixed brain was performed by sectioning the specimen in the coronal plane similar to that used for the postmortem MR imaging study. Petechial hemorrhages were present in the left uncus; however, the left parahippocampal gyrus was intact without a prominent groove, as would be expected in a significant temporal lobe herniation. Sections were notable for a 2.5-cm colloid cyst filling and distending the rostral third ventricle (Fig 3A). The lesion was wedged between the splayed columns of

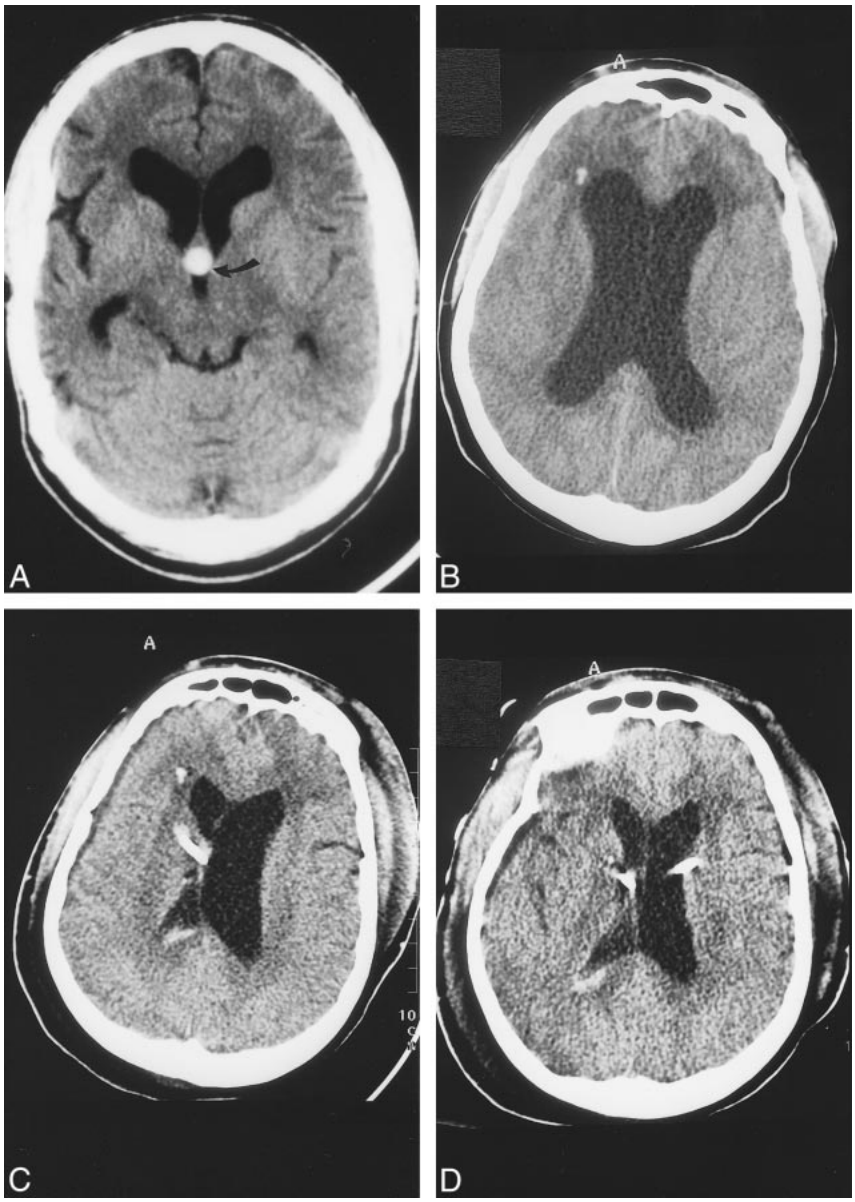

FIG 1. Baseline CT and CT studies obtained during present admission.

A, Baseline noncontrast axial 5-mm section shows hyperdense colloid cyst (*arrow*) in the rostral aspect of the third ventricle. There is moderate dilatation of the lateral ventricles and cerebral atrophy secondary to AIDS. In this view, the colloid cyst is round in appearance.

B, CT scan obtained immediately after acute neurologic deterioration shows marked hydrocephalus and hypodensity in the white matter of the frontal lobes. The etiology of the presumed punctate hemorrhage in the right frontal lobe is not known.

C, CT obtained immediately after the initial ventriculostomy shows a right-sided catheter that has decompressed the lateral ventricle. The left lateral ventricle remains enlarged and there is mild midline shift to the right. A small amount of blood is present in the right lateral ventricle secondary to catheter insertion.

D, CT done after insertion of left-side ventriculostomy shows decreased hydrocephalus, compared with *B,* and no midline shift.

the fornix and obstructed the foramina of Monro (Fig 3B). Symmetric ventriculomegaly was present. Sectioning of the cyst showed a viscid, murky substance, hardened after formalin fixation (Fig 3C). Microscopic evaluation of the colloid cyst disclosed an inner layer of low cuboidal-to-pseudostratified columnar epithelial cells with occasional ciliated and goblet cells, underlaid by a thin capsule of fibrous connective tissue (Fig 4). Cyst contents consisted of amorphous, faintly eosinophilc material that was strongly periodic acid-Schiff (PAS)–positive owing to the presence of glycogen and mucosubstances. Colloid material was negative for von Kossa and Prussian blue stains, excluding the presence of calcium and iron, respectively. Hemorrhage was not identified. Throughout cerebral white matter and deep gray nuclei were numerous microglial nodules with scattered multinucleated giant cells, a distinctive feature of HIV encephalitis. A lymphocytic meningitis was present.

Discussion

Colloid cysts of the third ventricle are rare lesions comprising 0.5–1% of primary brain tumors. Most reported cases occur in the third to fifth decades of life (3). The paucity of cases in infancy and childhood is notable (4). Up to 1994, only 37 cases in children had been described (5). Headache occurs in 68–100% of patients and is often the presenting symptom. Headaches are characterized as brief, lasting seconds to minutes, and are initiated, exacerbated, or relieved by a change in position (6). Although colloid cysts are histologically benign, they may obstruct the foramina of Monro and produce acute hydrocephalus. These lesions are a rec-

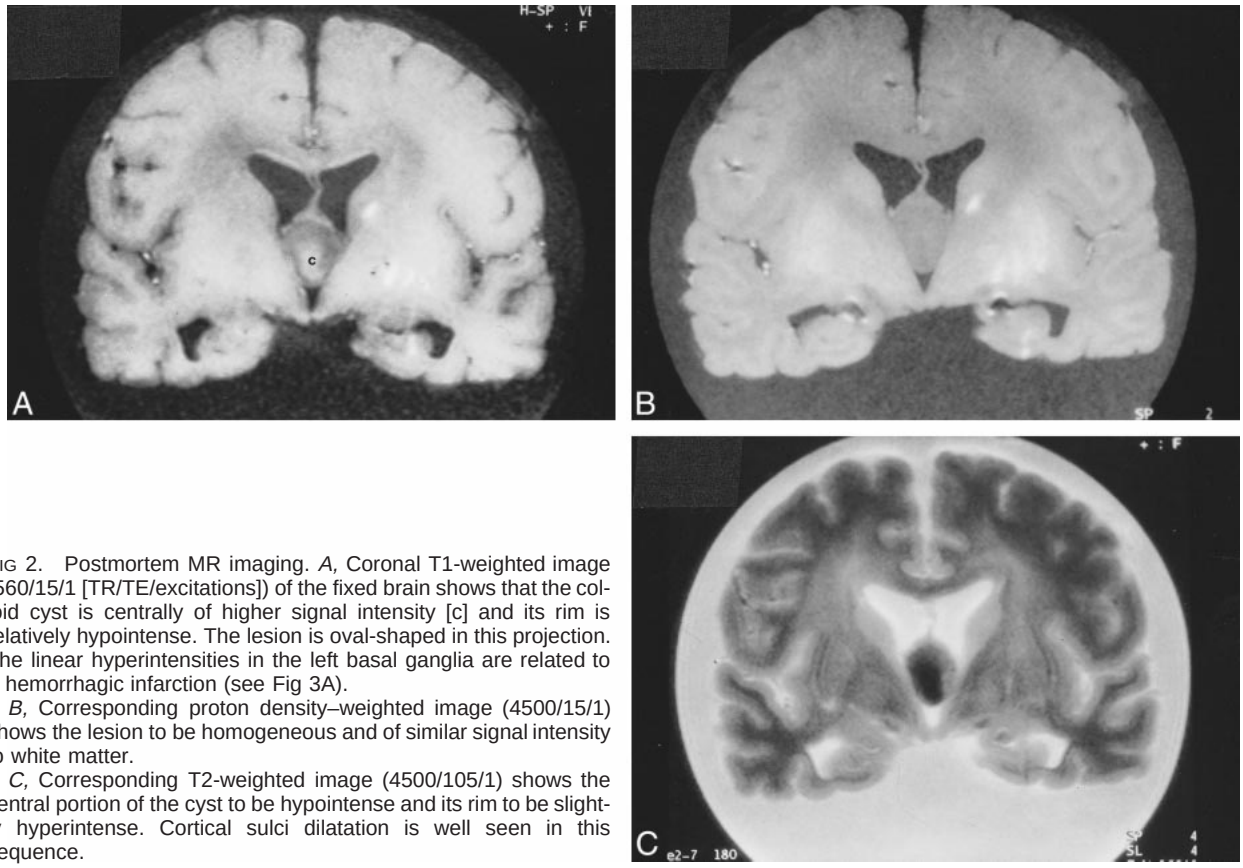

FIG 2. Postmortem MR imaging. *A,* Coronal T1-weighted image (560/15/1 [TR/TE/excitations]) of the fixed brain shows that the colloid cyst is centrally of higher signal intensity [c] and its rim is relatively hypointense. The lesion is oval-shaped in this projection. The linear hyperintensities in the left basal ganglia are related to a hemorrhagic infarction (see Fig 3A).

B, Corresponding proton density–weighted image (4500/15/1) shows the lesion to be homogeneous and of similar signal intensity to white matter.

C, Corresponding T2-weighted image (4500/105/1) shows the central portion of the cyst to be hypointense and its rim to be slightly hyperintense. Cortical sulci dilatation is well seen in this sequence.

ognized cause of sudden death (7). The cyst's attachment to the third ventricular roof may impart a pendulous character to the lesion, whereby foraminal obstruction may be intermittent. Some patients, upon awakening, complain of headache that is relieved by standing. Other symptoms include progressive dementia, drop attacks, and spells of transient loss of consciousness. In children, the most common symptoms are headache, nausea, vomiting, papilledema, and diplopia.

The smooth-walled, spherical cysts vary in size from 3–40 mm in diameter but may be larger. Cyst size does not appear to be a reliable predictor of outcome, as even small ones may result in sudden death (8). Although the great majority of colloid cysts arise in the anterior third ventricle, rare examples in the lateral ventricles, fourth ventricle and outside the ventricular system have been reported (9–11). Histologically, colloid cysts are characterized by a simple to pseudostratified epithelial lining with interspersed mucous goblet cells and scattered ciliated cells (Fig 4). The epithelium rests on a thin layer of connective tissue. The cyst content is PAS-positive and composed of amorphous material, sometimes showing necrotic leukocytes or cholesterol clefts or both.

The consistent site of origin in the anterosuperior aspect of the third ventricle belies the controversial histogenesis of colloid cysts. Traditional views, as expressed by Kappers in 1955 (12), favor its origin from either the diencephalic vesicle or the persistence of embryonic paraphysis. The human paraphysis develops as a pouchlike evagination of the diencephalic roof dorsal to the interventricular foramen in the 7th week of life. Paraphyseal rudiments normally disappear by total degeneration at approximately 3.5 months of age. Colloid cysts of the third ventricle may arise from detached, nondegenerating embryonic vesicular recesses. Shuangshoti, 10 years later, suggested that colloid cysts of the third ventricle were derived from neuroepithelium, including ependyma and choroid plexus, and favored the term ''neuroepithelial cyst'' (13). In 1992, using immunohistochemical techniques, Tsuchida et al (14) offered a nonneuroepithelial origin of colloid cyst epithelium, underscoring its similarity to respiratory mucosa of the trachea and sphenoid sinus. Ho and Garcia (15) found the following features upon ultrastructural analysis of colloid cysts: ciliated cells and nonciliated cells with microvilli, goblet cells with secretory granules, and basal cells and undifferentiated cells with scanty organelles. Specialized intercellular junctional complexes, or desmosomes, were noted in many cell types. Desmosomes are a characteristic feature of epithelial cells and promote cell cohesion. In the ultrastructural analysis of colloid cysts, both the type of cells and their topographic arrangement were reminiscent of respiratory epithelium, and thus, an endodermal lineage. (15) Owing to these endodermal features, it has been suggested that colloid cysts and Rathke cleft cysts may

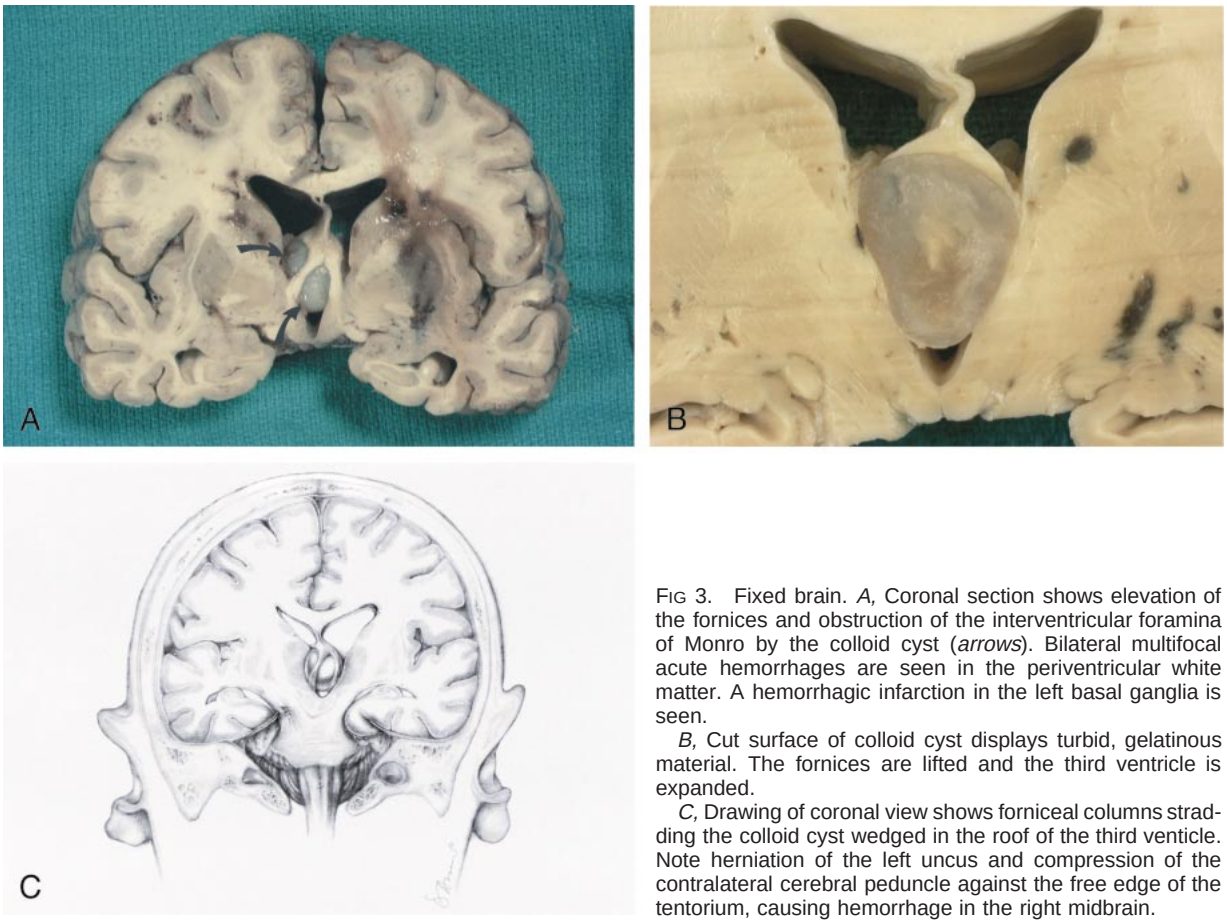

FIG 3. Fixed brain. *A,* Coronal section shows elevation of the fornices and obstruction of the interventricular foramina of Monro by the colloid cyst (*arrows*). Bilateral multifocal acute hemorrhages are seen in the periventricular white matter. A hemorrhagic infarction in the left basal ganglia is seen.

B, Cut surface of colloid cyst displays turbid, gelatinous material. The fornices are lifted and the third ventricle is expanded.

C, Drawing of coronal view shows forniceal columns straddling the colloid cyst wedged in the roof of the third venticle. Note herniation of the left uncus and compression of the contralateral cerebral peduncle against the free edge of the tentorium, causing hemorrhage in the right midbrain.

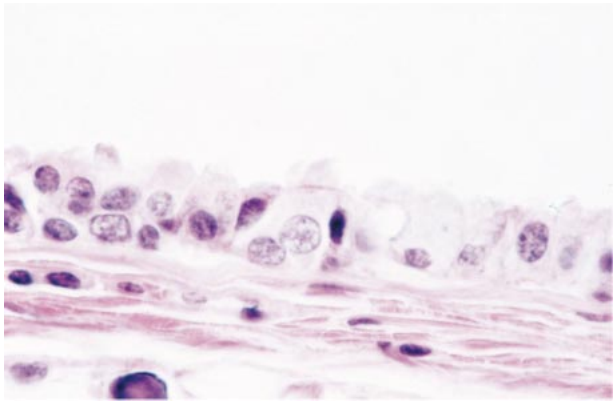

FIG 4. High-power microscopic image. View of the wall of the colloid cyst reveals epithelium with interspersed ciliated and goblet cells resting on collagenous tissue.

represent the same lesion in different locations (16).

Derived from the Greek word *kollodes* (''resembling glue''), the thick, gelatinous contents of colloid cysts are strongly PAS positive and are presumably derived from the secretions and breakdown products of the epithelial lining. Evidence of recent or remote hemorrhage and cholesterol crystals may be found. On occasion, chemical irritation resulting from hemorrhage, cholesterol, or the colloid material itself may give rise to a secondary xanthogranulomatous reaction within the cyst wall (17). Histologically, xanthogranulomatous reactions consist of numerous foamy cells, chronic inflammatory cells, epithelioid cells, and multinucleated giant cells (18).

Both CT and MR imaging may be used in the diagnosis of colloid cysts. On CT scans, most are slightly hyperdense with respect to the brain, but may occasionally be hypodense or isodense to it (2) (Fig 1). Most colloid cysts are oval or rounded. After administration of iodinated contrast material, a thin rim of enhancement may be present and is thought to represent the cyst capsule. Using MR imaging, colloid cysts have a variable appearance. MR imaging may occasionally show intracystic fluid levels or central and peripheral components in the lesion. Some colloid cysts are homogeneous in appearance. About 50% of colloid cysts are hyperintense on T1-weighted images, and the rest are either isointense or hypointense with respect to brain (Fig 5A). On T2-weighted images, most colloid cysts are hypointense to the brain (Fig 5B). Cysts that are hypointense on T2-weighted sequences may be difficult to visualize using fluid-attenuated inversion recovery images (FLAIR) (Fig 6A and B). Isointense cysts may be difficult to identify on MR images and may be more easily seen on CT scans (8). The T2 features of some

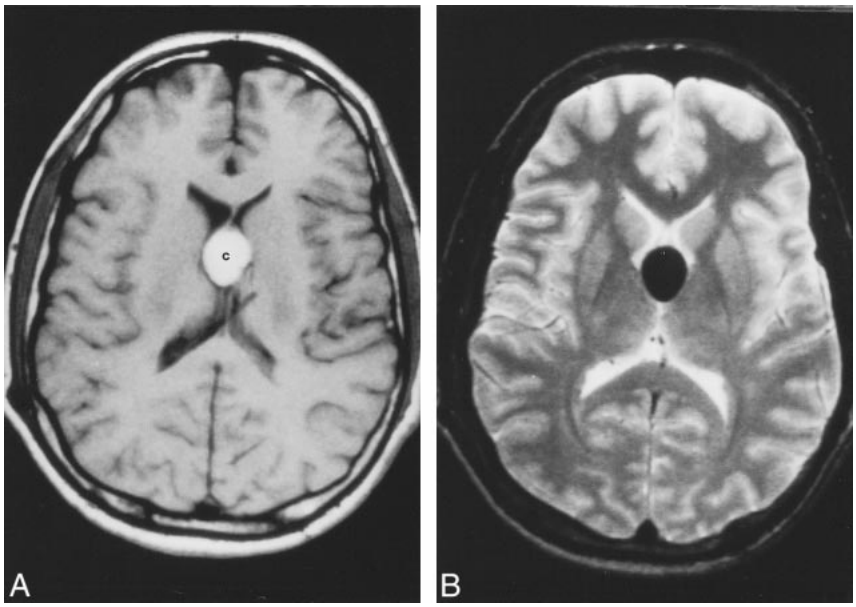

FIG 5. In vivo MR imaging of a colloid cyst (different patient).

A, Axial noncontrast T1-weighted image shows oval-shaped, hyperintense colloid cyst [c].

B, Corresponding T2-weighted image shows the cyst to be markedly hypointense. There is no hydrocephalus in this patient.

colloid cysts are the reversal of their pattern as seen on T1-weighted images (as shown in our patient). Because the central portion of most colloid cysts tends to be of low T2 signal intensity, it has been suggested that paramagnetic effects may be responsible for their MR imaging characteristics. Although iron was not found in our patient and has not been reported as being common inside colloid cysts, small quantities of this element may be present in macrophages found in the cyst wall. These macrophages are, however, not present in the central part of the cyst, which is the most hypointense on T2-weighted sequences. Calcifications are also rare in colloid cysts. We are aware of only one case report of a large colloid cyst with small mural calcifications (19). Thus, calcification cannot be invoked to explain MR imaging features of colloid cysts that are of low T1 and T2 signal intensity.

In one reported case, atomic emission spectrometry showed the presence of sodium, calcium, magnesium, and trace amounts of silicon, copper, iron, phosphorus, and aluminum (20). Because these compounds are found in minute quantities, they are not believed to be responsible for the imaging features of colloid cysts. Prompted by these observations, we obtained energy-dispersive X-ray microanalysis (EDX) of the contents of our patient's colloid cyst. Energy-dispersive systems are solid-state detectors with good energy resolution used in conjunction with a multichannel pulse amplitude analyzer. EDX spectrometers are used for accumulating spectra in short time intervals that permit a preliminary interpretation of the qualitative and quantitative chemical elemental composition of the specimen (21). In the present case, EDX analysis showed the presence of a significant amount of sulphur and only trace amounts of sodium and aluminum (Fig 7A). Initially we thought that the sulphur may have been due to long-term therapy and subsequent exposure of CNS tissue to sulpha-con-

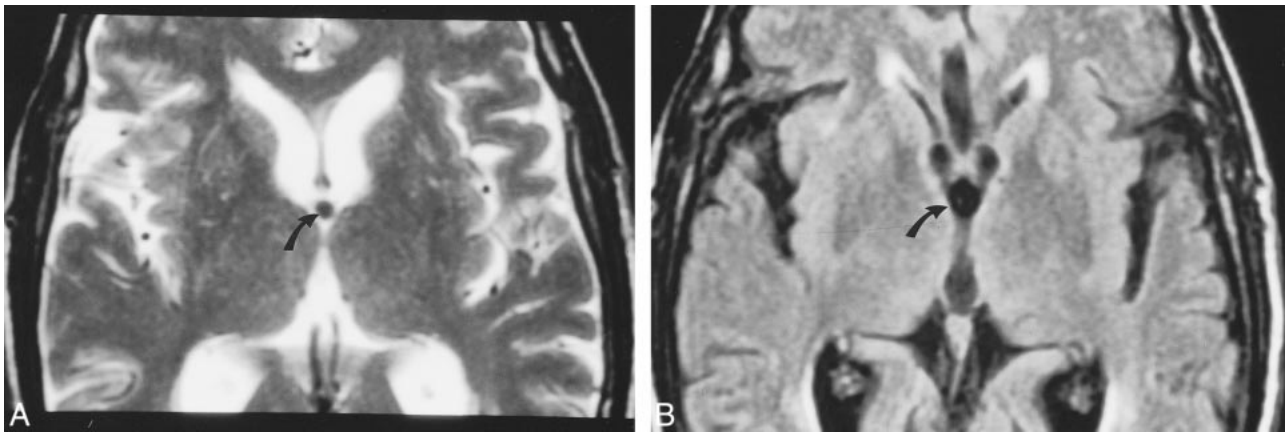

FIG 6. Colloid cyst imaged using FLAIR images (different patient).

A, Axial T2-weighted image shows small, rounded, hypointense colloid cyst (*arrow*) in the anterior aspect of the third ventricle.

B, FLAIR image obtained at nearly the same level shows that the colloid cyst (*arrow*) appears slightly larger than on *A* and is indistinguishable from the surrounding CSF.

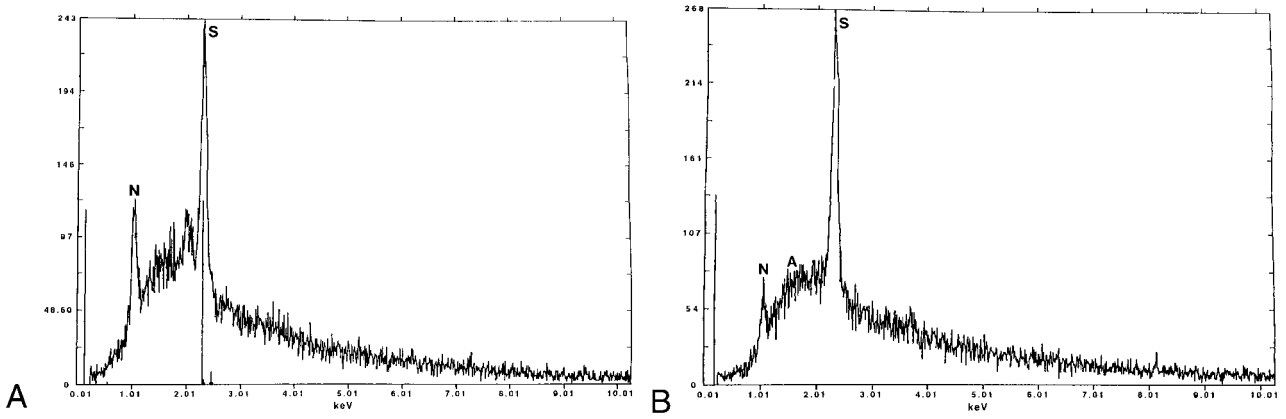

FIG 7. EDX of colloid cysts. *A,* Analysis of the contents of the entire colloid cyst shown in Figs 1–3 shows a large peak (S) corresponding to sulphur, and smaller peaks corresponding to sodium (N) and aluminum (A).

B, Analysis of the contents of a different colloid cyst shows large peak (S) of sulphur and also sodium (N). No paramagnetic substances are present in either cyst.

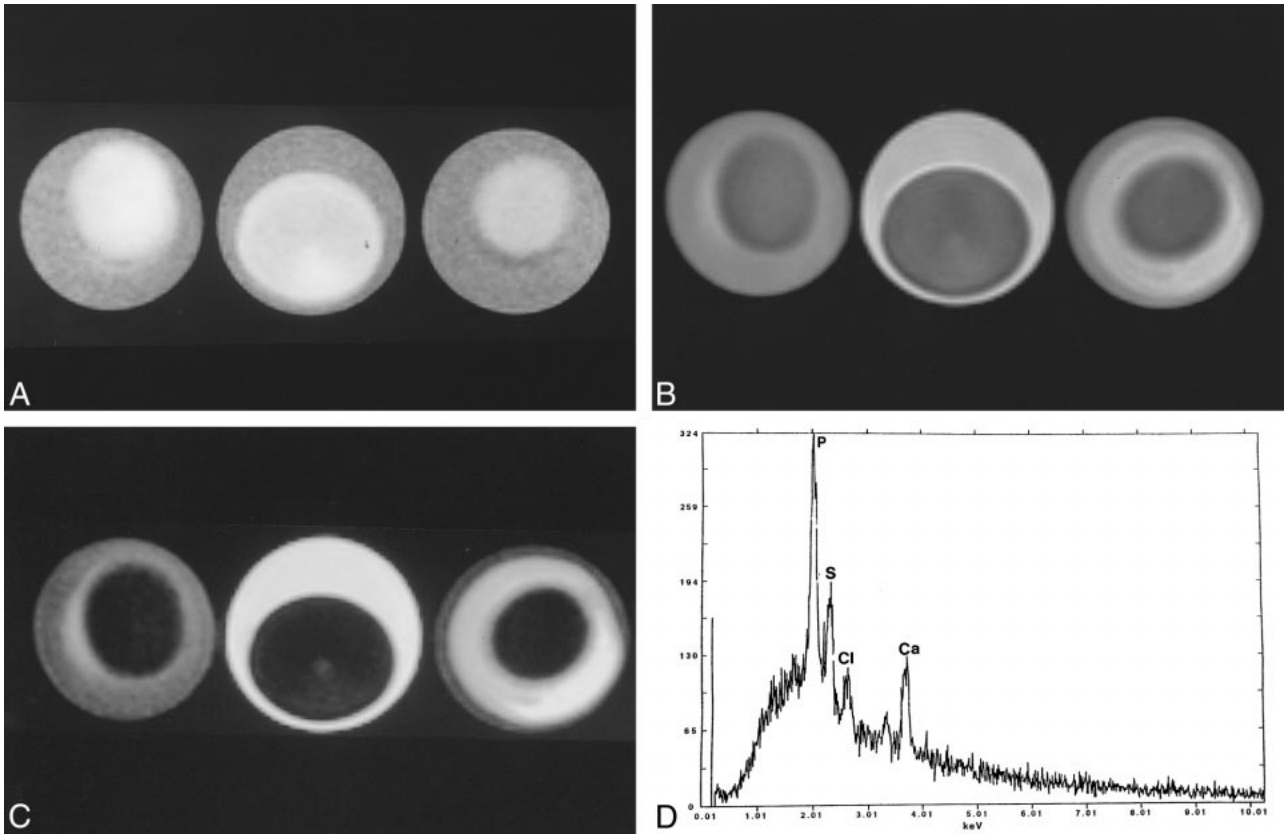

FIG 8. Egg phantom imaged using same parameters as those used for the postmortem brain imaging.

A, T1-weighted image of all three eggs (3-minute boiled [left], fresh [middle], and hard boiled [right]) show central relative hyperintensity corresponding to the yolk, the region of higher cholesterol content. The rim (*egg white*) is relatively hypointense and is probably related to high water content.

B, Corresponding proton density–weighted image shows that the yolk is hypointense with respect to the relatively hyperintense egg white.

C, Corresponding T2-weighted image shows that the yolk is hypointense with respect to the egg white. The egg white is brighter in the fresh egg and darker on the hard-boiled egg, probably reflecting the amount of free water it contains. The appearance of liquid, semisolid, and solid cholesterol is nearly identical in all sequences. Note that the imaging features of this phantom closely follow those seen in the postmortem study (Fig 3) and in some in vivo colloid cysts (Fig 5).

D, EDX analysis of a hard-boiled egg (mostly yolk) shows sulphur (S), chloride (Cl) and calcium (Ca). The large peak of phosphorus (p) is due to contamination of the yolk by egg white. There are no paramagnetic substances that could be responsible for the appearance of the eggs on MR imaging.

taining drugs used for the treatment of cerebral toxoplasmosis. Therefore, as a control, we performed EDX on the contents of a colloid cyst in a different patient without a history of sulpha-containing drug therapy, and found similar results (Fig 7B). The origin of the sulphur can only be speculated. Naturally occurring sulfhydryl-containing substances in the human body such as glutathione, cysteine, and cystine may be secreted by the cyst epithelium and may be at least partly responsible for the high sulphur content we observed. Because sulphur has no paramagnetic properties and other elements capable of this behavior were absent, we propose that it is the cholesterol esters contained in the cysts that are responsible for its MR imaging features. This has also been suggested by others (2). We used a fresh chicken egg, a 3-minute boiled egg, and a hard-boiled egg with the intention that the yolks would reflect liquid, semisolid, and solid cholesterol, respectively. We imaged these eggs by placing them over a water-filled cushion and found that using parameters typical of those also used in clinical MR imaging, they showed patterns identical to those seen in some colloid cysts (Fig 8A–C). Low T2 signal intensity was found in the yolk of all three eggs. We performed EDX in the egg and found no paramagnetic substances (Fig 8D). Thus it is possible that the MR imaging features of some colloid cysts are due to their cholesterol contents and not the presence of paramagnetic substances.

Understanding the imaging features of colloid cysts may have practical implications. It has been established that colloid cysts that are hypodense on CT scans may be aspirated successfully (22). A hyperdense CT appearance correlates with much more viscid contents and a failure of stereotatic aspiration. Similarly, a hypointense appearance on MR T2-weighted images may be used to predict a difficult aspiration and may direct these patients toward alternate surgical procedures. Microsurgical stereotatic techniques are now more popular than are conventional craniotomies for the treatment of colloid cysts (23). In one large series, microsurgical techniques produced excellent results in 30 of 33 patients (1). In patients admitted while deeply unconscious, even desperate therapies will not change their dismal outcome. Endoscopic cyst resection with monopolar or laser coagulation of its walls is also successful (24). After complete resection, cyst recurrence does not occur, but hydrocephalus may persist in up 30% of cases and require shunting. After incomplete resection, recurrence may occur in about 10% of patients. Complications from surgery include infarctions secondary to injury to the deep venous system and memory difficulties secondary to injury to the forniceal columns. The placement of permanent biventricular shunts offers a more conservative treatment choice for the management of these lesions. This option may be used for elderly patients and those refusing surgery.

Conclusion

Colloid cysts are rare lesions arising in the superior third ventricle and may present in acute hydrocephalus, which may be fatal. The origin of colloid cysts continues to be a matter of debate. Their MR imaging signal characteristics are variable and mostly dependent on the cholesterol and protein contents and not on the presence of paramagnetic minerals. Despite their variable signal characteristics, their location and shape allow for the correct preoperative diagnosis in most patients.

Acknowledgements

We thank Dr. Robert Bagnell for performing the EDX studies.

References

1. Hernesniemi J, Leivo S. **Management outcome in third ventricular colloid cysts in a defined population; a series of 40 patients treated mainly by transcallosal microsurgery.** *Surg Neurol* 1996;45:2–14
2. Maeder PP, Holtas SL, Basibuyuk LN, Salford LG, Tapper UAS, Brun A. **Colloid cysts of the third ventricle: correlation of MR and CT findings with histology and chemical analysis.** *AJNR Am J Neuroradiol* 1990;11:575–581
3. Bigner DD, McLendon RE, Bruner JM. ***Russell and Rubinstein's Pathology of Tumors of the Nervous System.*** 6th ed. London: Hodder Headline Group;1998:338–342
4. Zulch KJ. ***Brain Tumors.*** *Their Biology and Pathology*. 3rd ed. Berlin: Springer-Verlag;1986:519
5. Macdonald RL, Humphreys RP, Rutka JT, Kestle JRW. **Colloid cysts in children.** *Pediatr Neurosurg* 1994;20:169–177
6. Young WB, Silberstein SD. **Paroxysmal headache caused by colloid cyst of the third ventricle: case report and review of the literature.** *Headache* 1997;37:15–20
7. Chan RC, Thompson GB. **Third ventricular cysts presenting with acute neurological deterioration.** *Surg Neurol* 1983;19: 358–362
8. Mamourian AC, Cromwell LD, Harbaugh RE. **Colloid cyst of the third ventricle: sometimes more conspicuous on CT than MR.** *AJNR Am J Neuroradiol* 1998;19:875–878
9. Bertalanffy H, Kretzschmar H, Gilsbach JM, Ott D, Mohadjer M. **Large colloid cyst in lateral ventricle simulating brain tumor.** *Acta Neurochir* 1990;104:151–155
10. Jan M, Ba-Zeze V, Velut S. **Colloid cyst of the fourth ventricle: diagnostic problems and pathogenic consideration.** *Neurosurgery* 1989;24:939–942
11. Campbell DA, Varma TR. **An extraventricular colloid cyst; case report.** *Br J Neurosurg* 1991;5:519–522
12. Kappers JA. **The development of the paraphysis cerebri in man with comments on its relationship to the intercolumnar tubercle and its significance for the origin of cystic tumors in the third ventricle.** *J Comp Neurol* 1955;102:425–498
13. Shuangshoti S, Roberts MP, Netsky MG. **Neuroepithelial (colloid) cysts.** *Arch Path* 1965;80:214–223
14. Tsushida T, Hruban R, Carson B, Phillips PC. **Colloid cysts of the third ventricle: immunohistochemical evidence for non-neuroepithelial differentiation.** *Hum Pathol* 1992;23:811–816
15. Ho KL, Garcia JH. **Colloid cysts of the third ventricle: ultrasructural features are compatible with endodermal derivation.** *Acta Neuropathol* 1992;83:605–612
16. Graziani N, Dufour H, Figarella-Branger D, Donnet A, Bouillot P, Grisoli F. **Do the suprasellar neurenteric cyst, the Rathke cleft cyst and the colloid cyst constitute the same entity?** *Acta Neurochir* (Wien) 1995;133:174–180
17. Hadfield MG, Ghatak NR, Wanger GP. **Xanthogranulomatous colloid cyst of the third ventricle.** *Acta Neuropathol* (Berl) 1985; 66:343–346
18. Shuangshoti S, Phonprasert C, Suwanwela N, Netsky MG. **Combined neuroepithelial (colloid) cyst and xanthogranuloma (santhoma) in the third ventricle.** *Neurology* 1975;25: 547–552

19. Yuceer N, Baskaya M, Gokalp H. **Huge colloid cyst of the third ventricle associated with calcification in the cyst wall.** *Neurosurg Rev* 1996;19:131–133
20. Scotti G, Scialfa G, Colombo N, Landoni L. **MR in the diagnosis of colloid cysts of the third ventricle.** *AJNR Am J Neuroradiol* 1987;8:370–372
21. Parrish W, Mantler M. ***McGraw-Hill Encyclopedia of Science and Technology,* 8th ed.** New York: McGraw-Hill;1997:629–635
22. Kondziolka D, Lunsford LD. **Factors predicting successful stereotactic aspiration of colloid cysts.** *Stereotact Funct Neurosurg* 1992;59:135–138
23. Kyle l, Ross DA. **Stereotactic microsurgical craniotomy for the treatment of third ventricular colloid cysts.** *Neurosurgery* 1996; 38:301–307
24. Deinsberger W, Boker DK, Bothe HW, Samii M. **Stereotactic endoscopic treatment of colloid cysts of the third ventricle.** *Acta Neurochir* (Wien) 1994;131:260–264